University of Massachusetts Medical School

eScholarship@UMMS

Women's Health Research Faculty Publications

Women's Faculty Committee

2004-09-24

Smooth muscle archvillin: a novel regulator of signaling and contractility in vascular smooth muscle

Samudra S. Gangopadhyay

Et al.

Let us know how access to this document benefits you.

Repository Citation

Smooth muscle archvillin: a novel regulator of signaling and contractility in vascular smooth muscle

Samudra S. Gangopadhyay[1], Norio Takizawa[2], Cynthia Gallant[1], Amy L. Barber[1], Hyun-Dong Je[1], Tara C. Smith[2], Elizabeth J. Luna[2] and Kathleen G. Morgan[1,3,*]

[1]Boston Biomedical Research Institute, 64 Grove Street, Watertown, MA 02472, USA
[2]Cell Dynamics Group, Department of Cell Biology, University of Massachusetts Medical School, 55 Lake Avenue, Worcester, MA 01605, USA
[3]Department of Medicine, Beth Israel Deaconess Medical Center, Harvard Medical School, 330 Brookline Avenue, Boston, MA 02215, USA
*Author for correspondence (e-mail: morgan@bbri.org)

Summary

The mechanisms by which protein kinase C (PKC) and extracellular-signal-regulated kinases (ERK1/2) govern smooth-muscle contractility remain unclear. Calponin (CaP), an actin-binding protein and PKC substrate, mediates signaling through ERK1/2. We report here that CaP sequences containing the CaP homology (CH) domain bind to the C-terminal 251 amino acids of smooth-muscle archvillin (SmAV), a new splice variant of supervillin, which is a known actin- and myosin-II-binding protein. The CaP-SmAV interaction is demonstrated by reciprocal yeast two-hybrid and blot-overlay assays and by colocalization in COS-7 cells. In differentiated smooth muscle, endogenous SmAV and CaP co-fractionate and co-translocate to the cell cortex after stimulation by agonist. Antisense knockdown of SmAV in tissue inhibits both the activation of ERK1/2 and contractions stimulated by either agonist or PKC activation. This ERK1/2 signaling and contractile defect is similar to that observed in CaP knockdown experiments. In A7r5 smooth-muscle cells, PKC activation by phorbol esters induces the reorganization of endogenous, membrane-localized SmAV and microfilament-associated CaP into podosome-like structures that also contain F-actin, nonmuscle myosin IIB and ERK1/2. These results indicate that SmAV contributes to the regulation of contractility through a CaP-mediated signaling pathway, involving PKC activation and phosphorylation of ERK1/2.

Key words: Supervillin, Calponin, PKC, ERK, Podosome

Introduction

Stimulus-dependent protein scaffold formation is required for many intracellular signaling pathways, including those associated with protein kinases A and C (PKA and PKC), receptor tyrosine kinases, G-protein-coupled receptors, and integrins (Carpenter, 2000; Feliciello et al., 2001; Miller and Lefkowitz, 2001; Pryciak, 2001; Sim and Scott, 1999; Zamir and Geiger, 2001). Extracellular-signal-regulated kinases 1 and 2 (ERK1/2), and other members of the mitogen-activated protein kinase (MAPK) family are downstream in many of these signaling cascades and are also controlled by intracellular compartmentalization through interactions with scaffolding proteins (Ge et al., 2003; Pouysségur and Lenormand, 2003). Among the many effector pathways regulated by labile scaffold formation and localized signaling are the membrane and cytoskeleton rearrangements involved in cell translocation and contractility (Carpenter, 2000; Feliciello et al., 2001; Ge et al., 2003).

Although the signaling pathways that control contractility in differentiated smooth-muscle cells remain to be fully elucidated, both myosin-linked and actin-linked mechanisms are involved (Harnett and Biancani, 2003; Gerthoffer and Gunst, 2001; Pfitzer, 2001; Wier and Morgan, 2003; Gusev, 2001; Morgan and Gangopadhyay, 2001; Somlyo and Somlyo, 2003). Calcium ions bound to calmodulin regulate the contractility of smooth-muscle myosin II through activation of myosin-light-chain kinase (MLCK). However, tonic contractility in vascular smooth muscle does not necessarily correlate with myosin-light-chain phosphorylation (Jiang and Morgan, 1989; Moreland et al., 1992). Additional proposed regulatory targets include agonist-mediated activation of PKC and ERK1/2, and phosphorylation of the actin-binding protein caldesmon.

Calponin (CaP) was originally isolated from chicken gizzard (Takahashi et al., 1986) and has been proposed as an adapter protein in the actin-linked, agonist-induced regulation of contractility in smooth muscle (Gusev, 2001; Morgan and Gangopadhyay, 2001; Small and Gimona, 1998). Caldesmon and CaP compete with each other for binding to actin filaments in vitro and localize differently in vivo (for reviews, see Gusev, 2001; Small and Gimona, 1998; Wang, 2001). Caldesmon is found predominantly with actin filaments in the contractile apparatus, whereas CaP can localize with filamentous actin (F-actin) in the surrounding cortical cytoskeleton and membrane skeleton (Khalil et al., 1995; Parker et al., 1998). Thus, CaP is better situated to mediating membrane-associated contractile processes.

Antisense-mediated knockdown of CaP inhibits smooth-muscle contractility and ERK1/2 activation (Je et al., 2001). CaP binds directly to PKC and ERK1/2 (Leinweber et al., 1999; Leinweber et al., 2000). CaP also binds to F-actin and inhibits the actin-activated Mg ATPase of smooth-muscle myosin in vitro, an inhibition that can be reversed by phosphorylation of CaP (for a review, see Winder et al., 1998).

Upon agonist stimulation in vivo, CaP translocates and immunoprecipitates with ERK1/2 and PKC in differentiated smooth muscle (Menice et al., 1997).

Archvillin is a ~250-kDa membrane skeleton protein that localizes to cortical punctae in differentiating C2C12 cells and, with dystrophin, to costameres, which are sites of force transduction at the plasma membrane in striated muscle (Oh et al., 2003). Archvillin is a larger isoform of nonmuscle supervillin, which binds tightly to membranes, F-actin and smooth-muscle and nonmuscle myosin II (Chen et al., 2003; Pestonjamasp et al., 1995; Pestonjamasp et al., 1997). Supervillin is isolated with signaling and lipid-raft-organizing proteins from neutrophil plasma membranes, and has been implicated in the regulation of cell adhesion (Nebl et al., 2002; Pestonjamasp et al., 1997). Supervillin and archvillin both contain sequences that activate the transcriptional activity of the androgen receptor (Ting et al., 2002), and nuclear localization has been observed (Oh et al., 2003; Pestonjamasp et al., 1997; Ting et al., 2002). Overexpression of the muscle-specific archvillin sequences in differentiating C2C12 cells inhibits myotube formation, consistent with a dominant-negative effect during early myogenesis (Oh et al., 2003).

In this paper, we identify smooth-muscle archvillin (SmAV) as a unique isoform of supervillin (SV) that interacts with CaP. SmAV is most similar to, but is distinct from, skeletal-muscle archvillin. We discovered the CaP-SmAV association by yeast two-hybrid analyses with CaP as bait. The purposes of the present study were: (1) to confirm the CaP-SmAV interaction; and (2) to test whether SmAV contributes to the regulation of contractility through the CaP-mediated signaling pathway, which requires PKC activation and phosphorylation of ERK1/2.

The interaction was confirmed both by reciprocal blot overlays and by colocalization of CaP and C-terminal sequences of supervillin (c-SV) that lack the actin- and myosin-II-binding sites. CaP and c-SV colocalize to or near the plasma membrane after overexpression in COS-7 cells and before and after permeabilization with detergent. CaP and SmAV colocalize at endogenous levels to the cortices of freshly isolated smooth-muscle cells, after agonist stimulation. Antisense knockdown of SmAV expression decreases PKC-activated contractility and phosphorylation of ERK1/2, signaling effects similar to those observed previously for a CaP knockdown in this system (Je et al., 2001). SmAV, CaP and ERK1/2 localize with F-actin and nonmuscle myosin IIB to PKC-induced 'podosome-like' structures in A7r5 smooth-muscle cells, suggesting that these structures represent sites of CaP- and SmAV-mediated signaling. Taken together, our results show that SmAV is an essential regulator of contractility in differentiated smooth muscle and suggest that SmAV acts in concert with CaP, PKC and ERK1/2 in the plasma membrane cortex subsequent to agonist stimulation.

Materials and Methods

Yeast two-hybrid screening

CaP cDNA (Je et al., 2001) was cloned into the bait vector pBD-GAL4 Cam (Stratagene, La Jolla, CA). A HybriZAP® 2.1 two-hybrid ferret aorta cDNA library was constructed as described (Je et al., 2001), excised from phage and transformed into yeast strain YRG-2 containing the bait vector. Transformants with target plasmids were screened for histidine prototrophy and for β-galactosidase activity according to the manufacturer's instructions (Stratagene). Interacting plasmid DNA (pAD-GAL4-2.1-c-SmAV) was isolated from a positively interacting colony and identified by DNA sequencing and BLAST search. To confirm the interaction of CaP and the C-terminus of SmAV, the bait and prey were exchanged. CaP cDNA was cloned into pAD-GAL4-2.1 vector (pAD-GAL4-2.1-CaP) and the cDNA of c-SmAV was cloned into pBD-GAL4 Cam vector (pBD-GAL4 Cam-c-SmAV). The deletion constructs of CaP were made by PCR amplification of the cDNA residues corresponding to amino acids 1-136 and 1-163. They were cloned into the pAD-GAL4-2.1 vector (pAD-GAL4-2.1-Cap136 and pAD-GAL4-2.1-CaP163, respectively).

Reverse-transcription PCR

For reverse-transcription PCR (RT-PCR) cDNA was made from random-primed total ferret aorta RNA (1 μg) generated with the Advantage RT-for-PCR kit (BD Biosciences Clontech, Palo Alto, CA) and diluted to 100 μl. PCR amplification was performed with two sets of primers: MSV-F1 (5′-YTGCACTYCCTAAAGYTGCAGAAT-TAAGAMAAAT-3′) with CRATY-R (5′-ACACGTAAACTTCAC-TACCAAAGTCAAACACCAG-3′); and C (5′-GTCCCTGATGAC-GACTACTGGGGG-3′) with D (5′-AACTGCTGAGGATGAA-CAGGCGGG-3′). Amplifications were performed using a PTC-100 thermocycler (MJ Research, Waltham, MA) and a program as follows: 92°C for 2 minutes (1 cycle); 92°C for 30 seconds, 68°C for 8 minutes (5 cycles); 92°C for 30 seconds, 63°C for 30 seconds, 70°C for 8 minutes (5 cycles); 92°C for 30 seconds, 57°C for 30 seconds, 70°C for 8 minutes (30 cycles); and 70°C for 10 minutes (1 cycle). The reaction was then held at 10°C overnight. The amplified products were cloned and sequenced in both directions.

Expression constructs

A glutathione-S-transferase (GST) expression construct encoding the C-terminal 251 amino acids of SmAV (GST-c-SmAV) was generated by directionally ligating the two-hybrid target vector into the EcoRI/XhoI sites of pGEX-6P-1 (Amersham Pharmacia Biotech, Arlington Heights, IL). Similarly, a chimera of GST and the C-terminal 510 amino acids of bovine supervillin (accession number AF025996; GST-c-BSV) was generated by ligating a partial cDNA into the SmaI/NotI sites of pGEX-6P-3. Recombinant His-tagged ferret h1 CaP was constructed by PCR amplification of the open reading frame (Je et al., 2001) with oligonucleotide primers containing BamHI (sense) and HindIII (antisense) restriction sites. Amplified products were inserted in frame into BamHI/HindIII-digested pET 30b vector (Novagen, Milwaukee, WI) for bacterial expression and into the pCDNA4/HisMax TOPO vector (Invitrogen Life Technologies, Baltimore, MD) for expression in COS-7 cells. Construction of EGFP-c-SV (EGFP-SV1010-1792) has been described (Wulfkuhle et al., 1999).

Purified proteins

Recombinant His-tagged ferret h1 CaP was expressed after IPTG induction of BL21 (DE3) Escherichia coli and purified using a Talon spin column (BD Biosciences) in the presence of 8 M urea. Purified protein was dialysed against 20 mM Tris HCl, pH 8.0, 100 mM NaCl, 10% glycerol and clarified by centrifugation. GST fusion proteins were expressed similarly in BL21(DE3)LysS cells and affinity purified on glutathione-Sepharose™ (Swaffield and Johnston, 2003). Proteins were eluted with 10 mM glutathione and dialysed against 20 mM MOPS, pH 7.5, 2 μg ml⁻¹ leupeptin, 60 mM KCl, 0.1% β-mercaptoethanol and 0.1 mM EGTA. Samples were frozen quickly in liquid nitrogen and stored at –80°C. Turkey-gizzard CaP purification and subsequent digestion with chymotrypsin were performed as previously described (Leinweber et al., 2000).

Antibodies

Mouse monoclonal anti-h1CaP antibody (Sigma Chemical, St Louis, MO) was used at 1:5000 for COS-7 cell experiments and at 1:20,000 with aortic cells. The rabbit polyclonal antibody against the first 340 residues of human supervillin (anti-H340) (Oh et al., 2003) was used at 1:10,000 dilution for immunoblotting and cell staining. Other rabbit polyclonal antibodies were used as follows: anti-green-fluorescent-protein (anti-GFP) (Santa Cruz Biotechnology, Santa Cruz, CA), 1:2000; anti-p44/42 MAPK/ERK1&2 (Cell Signaling Technology, Beverly, MA), 1:500; and anti-phospho-p44/42 MAPK/pERK1&2 (Cell Signaling Technology), 1:2000 dilution. Secondary antibodies used in immunofluorescence microscopy were from Molecular Probes (Eugene, OR) as follows: Oregon-green-conjugated goat anti-mouse and Rhodamine-Red-X-conjugated goat anti-rabbit for smooth-muscle cells; Rhodamine-Red-X-conjugated goat anti-mouse and Oregon-green-conjugated goat anti-rabbit for COS-7 cells; and Alexa-488-conjugated goat anti-rabbit and Texas-Red-conjugated goat anti-mouse for A7r5 cells.

COS-7 cells

COS-7 cells were grown to 90-95% confluence in six-well plates with Dulbecco's modified Eagle's medium containing 10% fetal bovine serum. Each well was transfected with 10 μg plasmid DNA (10 μg each for double transfections) in Lipofectamine 2000 reagent (Invitrogen). After a 48-hour incubation at 37°C, cells were trypsinized, plated onto coverslips and incubated for another 4 hours at 37°C. Coverslips were washed with PBS and fixed with 2% paraformaldehyde, permeabilized with 0.1% Triton X-100, blocked with 10% goat serum and reacted with primary and secondary antibodies. In some experiments, cells were pre-permeabilized with 0.1% or 0.5% Triton X-100 before fixation.

Ferret aorta cell isolation

Ferrets (Marshall Farms, North Rose, NY) were euthanized by an overdose of chloroform and abdominal aortas were excised quickly to a dish containing oxygenated physiological saline solution (PSS; 120 mM NaCl, 5.9 mM KCl, 25 mM NaHCO$_3$, 11.5 mM dextrose, 2.5 mM CaCl$_2$, 1.2 mM MgCl$_2$ and 1.2 mM NaH$_2$PO$_4$, pH 7.4). All procedures were approved by the Boston Biomedical Research Institute Animal Care and Use Committee. Single aorta cells were isolated using a variation of a previously described method (Menice et al., 1997). Each 100 mg of aorta (wet weight) were digested with medium A, which is composed of 1.2 mg CLS 2 collagenase (type II, 390 U mg^{-1}, lot number MIE4817; Worthington Biochemical, Lakewood, NJ) and 1.6 mg elastase (4.0 U mg^{-1}; Boehringer Mannheim, Indianapolis, IN) in a final total volume of 7.5 ml Ca- and Mg-free Hanks' balanced salt solution with 0.2% bovine serum albumin (BSA). Tissue pieces were incubated in a shaking water bath at 34°C for 90 minutes, filtered on a nylon mesh, rinsed and incubated for 20 minutes in digestion medium B (medium A with only 0.74 mg elastase). Tissue pieces were filtered, rinsed and reincubated in digestion medium C [medium B plus 0.5 mg of 5000 U soybean trypsin inhibitor (type II-S; Sigma)]. For all experiments, cells on one coverslip were tested to confirm that they shortened in response to phenylephrine. Cells were fixed and stained for immunofluorescence as described for COS-7 cells. To prevent cell shortening during phenylephrine-induced stimulation, both stimulated and unstimulated cells were placed in a Hanks' solution to which 300 mM sucrose was added to increase tonicity, as previously described (Khalil et al., 1995; Parker et al., 1998). This procedure has been shown not to interfere with signal transduction in smooth-muscle cells, as measured by agonist-induced increases in intracellular calcium concentration and by translocation of CaP and PKC, and is thought to prevent contraction directly at the cross-bridge level (for review, see Parker et al., 1998).

Imaging

COS-7 and aorta cells

Images were obtained with a Kr/Ar laser (Radiance 2000, BioRad Laboratories) scanning confocal microscope equipped with Nikon 60× (NA 1.4) or 40× (NA 1.4) oil immersion objective. Images were recorded and quantified with Laser Sharp 2000 (BioRad Laboratories) for Windows NT. Ratio analyses of fluorescent intensity distributions were performed as described (Khalil et al., 1994). The 'surface' fluorescence value was defined as the peak pixel intensity over the outer cell surface, and the 'cytoplasmic' value was taken as the peak value in the core of the cell (see Fig. 8, inset). Each ratio was the mean of values from three line scans from non-nuclear areas of each cell.

A7r5 cells

A7r5 cells were stimulated for 2 hours with 1 μM phorbol dibutyrate (PDBu; Sigma), washed once with pre-warmed PBS, pH 7.4, and fixed in 4% paraformaldehyde. Cells were permeabilized for 10 minutes with 0.1% Triton X-100 and blocked for 30 minutes in 1% BSA, 0.5% Tween-20, 0.02% sodium azide in PBS. Endogenous levels of SmAV, myosin IIB, ERK1/2, and CaP were visualized with 1:100 dilutions of rabbit polyclonal anti-H340 (Nebl et al., 2002), rabbit polyclonal anti-myosin IIB (Babco-Covance), rabbit polyclonal anti-ERK1/2 (UBI) and/or mouse monoclonal anti-CaP (clone hCaP; Sigma), respectively. F-actin was stained with a 1:1000 dilution of Texas-Red-conjugated phalloidin (Molecular Probes). Images were obtained with OpenLab software (Improvision, Lexington,MA) on a Zeiss Axioskop fluorescence microscope.

Colocalization analysis

The degree of colocalization between pairs of stained proteins in COS-7 cells and aorta smooth-muscle cells was quantified by a modification of a previously published method (Parker et al., 1998) and by using LaserPix image software (BioRad Laboratories). Images were thresholded to eliminate background signal outside cell boundaries. A colocalization coefficient between red and green fluorophores (C_{R-G}) was computed as,

$$C_{R-G} = \frac{\Sigma R_{i,coloc}}{\Sigma R_i},\qquad(1)$$

where the denominator is the sum of red pixels intensities greater than the threshold and the numerator is the sum of the intensities of red pixels that are greater than threshold and that also have a green component. The amount of reverse colocalization [i.e. (C_{G-R})] was computed in a similar manner by replacing the denominator of Eqn 1 with the sum of intensities of green pixels that are greater than the threshold. The colocalization coefficients are, by definition, between 0 and 1. A value of 0 indicates no colocalization and a value of 1 indicates complete colocalization.

The pixel intensities in each image were randomized by reading the pixel information within each image into a mathematical matrix. The elements of each matrix were then assigned to new locations within the matrix using a random number generator. After converting the randomized matrices back into images, the colocalization coefficients between the pair of random images were computed. A comparison of the colocalization coefficients for the random images to that for the original images allows an assessment of the degree to which colocalization between a pair of fluorophores was due to chance.

Tissue fractionation

Aortic ferret tissue was equilibrated for 1 hour at room temperature in oxygenated (95% O$_2$, 5% CO$_2$) PSS. Viability was tested with a depolarizing solution consisting of PSS in which 51 mM NaCl was stoichiometrically replaced by KCl. The tissue was further incubated

for 1 hour in PSS and quickly frozen in a dry-ice/acetone/ dithiothreitol slurry in either the presence or the absence of 10 μM phenylephrine for 10 minutes. Tissue was pulverized and homogenized at 4°C with 3 ml buffer I (20 mM Tris HCl, pH 7.5, 50 mM NaCl, 250 mM sucrose, 10 mM dithiothreitol (DTT), 3 mM EGTA, 5 mM MgCl$_2$, 1 mM ATP and protease inhibitors) (Je et al., 2001). Homogenized tissue was centrifuged at 165,000 *g* for 1 hour and the supernatant collected as the cytosolic fraction. The pellet was shaken for 1 hour at 4°C in 3 ml buffer II (20 mM Tris HCl, pH 7.5, 250 mM sucrose, 0.5% Triton X-100, 10 mM DTT, 3 mM EGTA, 5 mM MgCl$_2$, 1 mM ATP and protease inhibitors) and centrifuged at 165,000 *g* for 1 hour. This supernatant was collected as the Triton-extractable ('membrane') fraction. The pellet was resuspended in 3 ml buffer III [20 mM Tris HCl, pH 7.5, 250 mM sucrose, 0.5% Triton X-100, 1.2% sodium dodecyl sulfate (SDS), 10 mM DTT, 3 mM EGTA, 5 mM MgCl$_2$, 1 mM ATP and protease inhibitors], extracted at 4°C for 1 hour and centrifuged at 165,000 *g* for 1 hour. This final supernatant was collected as the Triton-resistant ('cytoskeletal') fraction.

Western blots

Tissue homogenate (25 μg) was loaded onto 4-15% Tris-HCl gradient gels (Bio-Rad Laboratories) and electroblotted onto PVDF membranes (Millipore, Billerica, MA). Blots of purified proteins were resolved on 4-15% gradient polyacrylamide gels (Laemmli, 1970) and electrotransferred to PVDF (Schleicher & Shuell, Keene, NH). Blots were blocked with 5% nonfat dried milk and incubated with primary and secondary antibodies. Signals were visualized by enhanced chemiluminescence. PBDu-treated A7r5 cells (1×10^6) were treated with 10% trichloroacetic acid and centrifuged at 10,000 *g* for 10 minutes at 4°C. The pellets were dissolved with 0.5 M NaHCO$_3$ and Tris base to adjust pH. Samples (1.5×10^5 cells per 4-mm lane) were resolved on 6-20% gradient polyacrylamide gels and transferred to nitrocellulose, as above. Blots were washed with TBS containing

0.05% Tween 20 and incubated for 1 hour with primary antibodies at room temperature. Signals were visualized with SuperSignal® WestPico (Pierce, Rockford, IL) after a 1-hour incubation with secondary antibodies conjugated with horseradish peroxidase.

Overlay assay

Equal amounts of proteins were resolved on SDS-polyacrylamide gels and transferred to PVDF membranes. Relative protein content was confirmed by naphthol blue black (NBB) staining of the membrane before incubation with the overlay solution. Blots were blocked with 5% milk in TBS and incubated for 1 hour with 1.25 μg ml^{-1} recombinant ferret CaP, GST-c-SmAV or GST in 154 mM NaCl, 10 mM Tris HCl, pH 7.4, 10 mg ml^{-1} BSA and protease inhibitors (Leinweber et al., 1999). Blots were fixed with 0.5% paraformaldehyde in PBS, neutralized with 2% glycine in PBS, washed six times with PBS and immunostained as for western blots.

Antisense knockdown of SmAV expression in smooth-muscle tissue

Experiments were performed as previously described (Kim et al., 2000). The antisense oligonucleotide used was 5′-CCTTGC-CAGAGGTACACCTCAT-3′, corresponding to amino acids HEVYLWQG (residues 1912-1919) of SmAV. A randomized version of this sequence (5′-CACTAGAGTCCAGCTACGCTCT-3′) served as the negative control. BLAST searches confirmed a lack of homology to any other relevant coding sequences. Nucleotides were phosphorothioated to minimize degradation and FITC tagged at their 5′ ends. Oligonucleotides were loaded once each day until day 4, as described previously (Je et al., 2001). Fluorescence microscopy at the end of each experiment confirmed internalization of the oligonucleotide into all cells of the tissue (Je et al., 2001). Contractility of the muscle strips was measured daily in response to
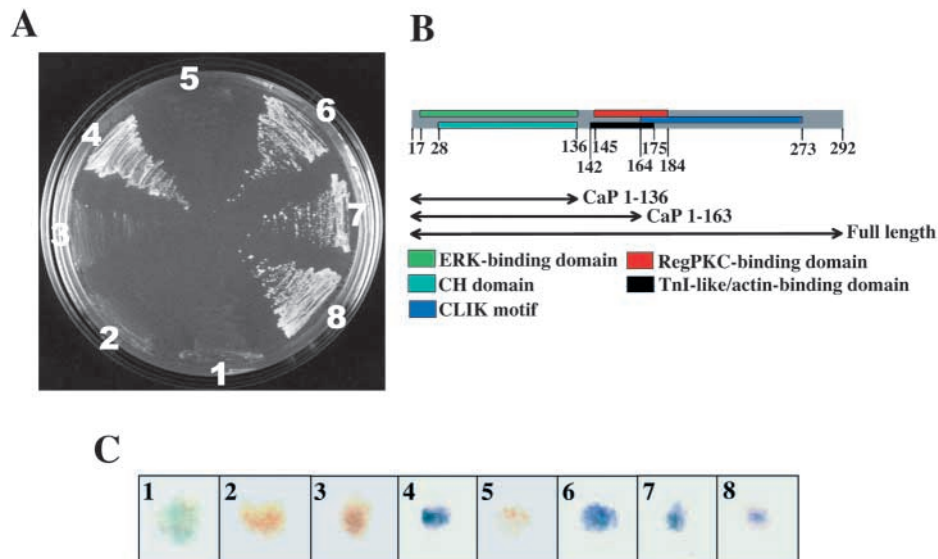
Fig. 1. Identification of SmAV as a CaP interacting protein. (A) Interactions between SmAV and CaP in reciprocal yeast two-hybrid assays. The growth of yeast host (YRG2) with plasmids or constructs in Trp-, Leu- and His-depleted selective medium. (1) Yeast Host-YRG2. (2) pBD-GAL4 Cam. (3) pBD-GAL4 Cam-CaP. (4) pBD-GAL4 Cam-CaP and pAD-GAL4-2.1-c-SmAV. (5) pBD-GAL4 Cam-c-SmAV. (6) pBD-GAL4 Cam-c-SmAV and pAD-GAL4-2.1-CaP. (7) pBD-GAL4 Cam-c-SmAV and pAD-GAL4-2.1-Cap136. (8) pBD-GAL4 Cam-c-SmAV and pAD-GAL4-2.1-CaP163. (B) CaP domains indicating the amino acid residue numbers (ferret sequence) and the domains (Morgan and Gangopadhyay, 2001). Double-headed arrows indicate the deletion constructs used. (C) Expression of LacZ as detected by blue color development with X-gal. Colonies of yeast cells (either host only or transfected with plasmid/constructs) are numbered as in (A).

51 mM KCl. No significant decreases in the amplitude of contraction to KCl were observed over the 4 day course of the experiment. The SmAV expression level and ERK1/2 phosphorylation levels were measured by densitometry of western blots from day 4 tissue extracts.

Statistics

Unless otherwise noted, significance of difference between means was taken at $P > 0.05$ by a two-tailed Student's t test.

Results

Identification of SmAV as a CaP-interacting protein

We used reciprocal yeast two-hybrid screens to identify a new interaction partner for CaP. We initially used the cDNA encoding ferret (h1) basic CaP as bait in an untargeted screen of a ferret aorta cDNA library. Out of thousands of transformants, one specific interacting clone was identified and verified (Fig. 1A,C4). This plasmid contained an 862-bp insert encoding 251 amino acids. A BLAST search of protein
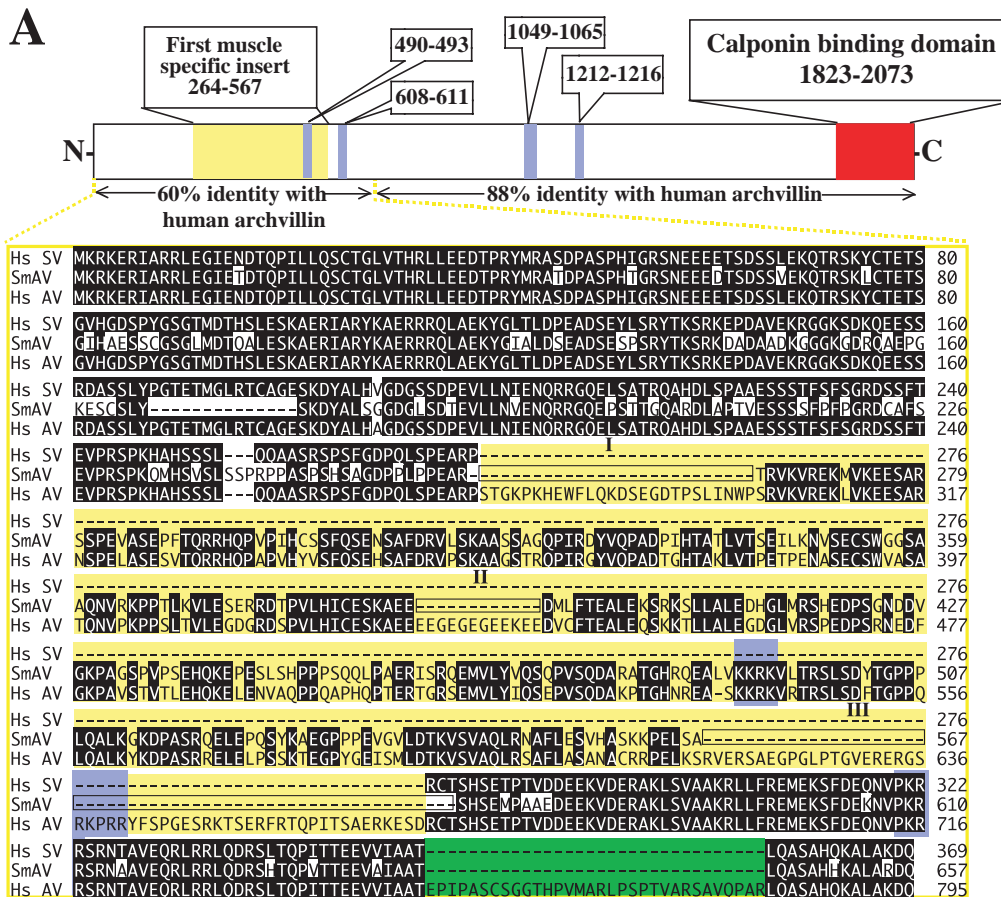
Fig. 2. Sequence comparisons of SmAV with human supervillin and archvillin. (A, top) The SmAV sequence. The muscle-specific sequence (insert 1) is in yellow (Oh et al., 2003) and the nuclear targeting sequences is in blue. The CaP-binding domain is represented by the red box. (A, bottom) The alignment of N-terminal amino acid sequences of ferret SmAV with those of human supervillin and human archvillin. Identical residues are in black; the second muscle-specific insert in skeletal-muscle archvillin is in green. The three sequences in skeletal-muscle but not smooth-muscle archvillin are boxed and numbered. Residue numbers are given on the right. The SmAV sequence data are available from GenBank (accession number AY380816). (B) Domain analysis of SmAV, based on homology with domains in supervillin (Chen et al., 2003) and motif searching programs (http://scansite.mit.edu/, http://www.ncbi.nlm.nih.gov/). Domains are marked with residue numbers. Sequences corresponding to the predicted binding sites for myosin II (lavender) and F-actin (brown) are shown. The CaP-binding domain is represented by the red box.
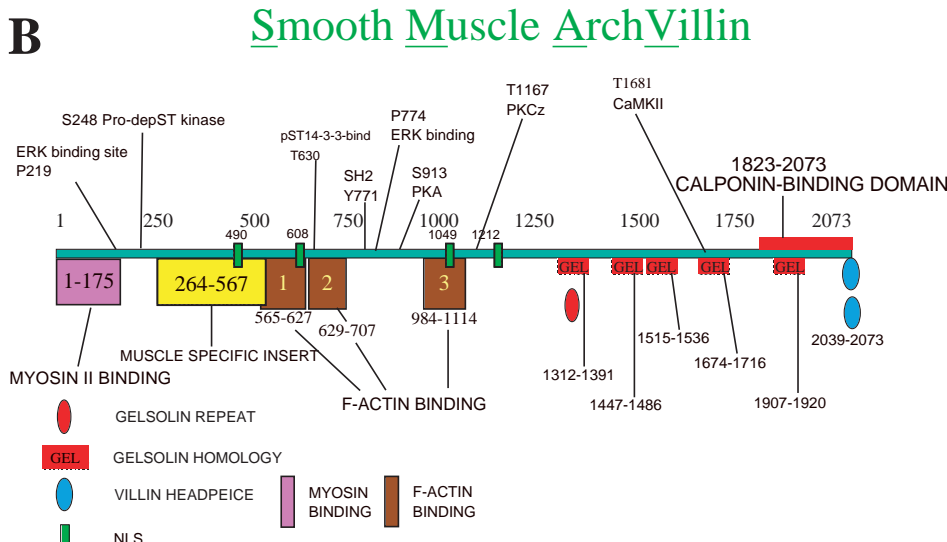
databases (Altschul et al., 1997) showed 94% identity with human supervillin. In the reciprocal experiment, the supervillin homolog in the bait vector also interacted with CaP as prey (Fig. 1A,C6). A deletion mutant (CaP 1-163) lacking the CLIK motif (Gimona et al., 2003) of CaP (Fig. 1B) interacted with the supervillin homolog (Fig. 1A,C8), as did a further deletion mutant (CaP 1-136) lacking both the TnI-Like domain and the CLIK motif but containing the single type 3 calponin homology (CH) domain (Gimona et al., 2002) of calponin (Fig. 1A,C7). The CH domain of CaP is of interest because it has also been identified as an ERK-binding domain (Leinweber et al., 1999).

The complete cDNA sequence for the supervillin-related protein in ferret aorta revealed a new splice variant that might be characteristic of smooth muscle. The encoded protein (Fig. 2) is predicted to exhibit a relative molecular mass of 231,457.96 and an isoelectric point of 6.44 (http://us.expasy.org/tools/pi_tool.html). The CaP-binding sequence initially identified by the yeast two-hybrid assay is the C-terminal 251 residues (1823-2073). Alignment with previously described supervillin family members revealed 82% similarity (78% identity) with human archvillin and 78% similarity (74% identity) with human supervillin. The C-terminal 1416 residues are 88% identical to the corresponding sequence of both supervillin and archvillin.

Archvillin, a skeletal-muscle-specific isoform of supervillin, contains two muscle-specific inserts encoded by four differently spliced exons in both human and murine tissues (Oh et al., 2003). The first muscle-specific archvillin insert is encoded by exons 3, 4 and 5 in skeletal muscle archvillin (Fig. 2A, yellow). The large exon 4 is conserved in the smooth-muscle archvillin protein sequence (residues 264-567), except for a short hypervariable region (Fig. 2A, region II). However, muscle insert sequences encoded by exons 3 and 5 are absent (Fig. 2A, regions I,III), as is the second muscle-specific archvillin insert (Fig. 2A, green), which is encoded by exon 9 in murine and human archvillins (Oh et al., 2003). Because of the greater similarity to skeletal-muscle archvillin, we have named the protein found in aortic smooth muscle SmAV for smooth-muscle archvillin. Thus, SmAV is intermediate in amino acid sequence between skeletal-muscle archvillin and non-muscle supervillin, presumably owing to alternative exon splicing.

The binding sites for myosin II and F-actin that have been recently mapped within the N-terminus of bovine supervillin (Chen et al., 2003) appear to be present and highly conserved within SmAV. SmAV contains a site from residues 1 to 175 (Fig. 2B, pink) with 80% identity to the binding site for non-muscle and smooth-muscle myosin II in supervillin. Similarly, residues 565-627, 629-707 and 984-1114 (Fig. 2B, brown) contain residues with 97%, 93% and 91% identity, respectively, to the three actin-binding domains of supervillin.
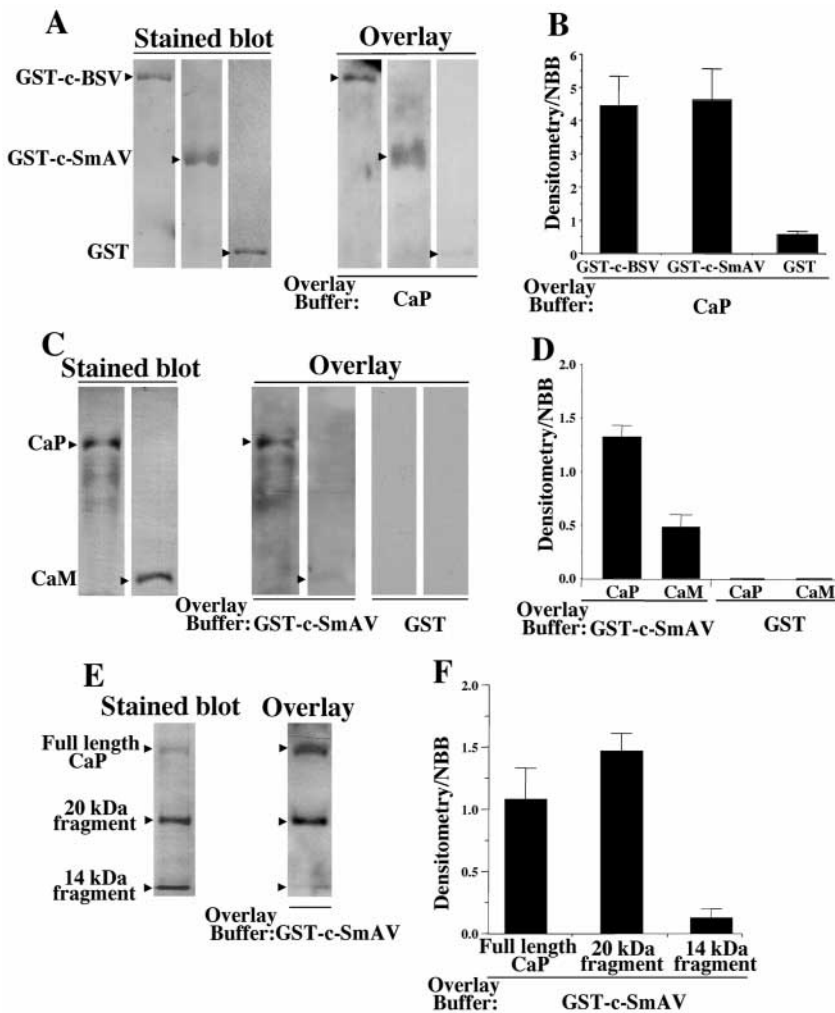
Fig. 3. Overlay analysis of binding interactions between CaP and supervillin/archvillin fragments. (A, left) Naphthol blue black (NBB) stain of total protein on blot before incubation with overlay solution. (A, right) Immunostain with anti-CaP antibody after processing with overlay buffer containing 1.25 μg ml^{-1} CaP. Purified proteins and their corresponding overlay signals in lanes are indicated with arrowheads. All three proteins were loaded at 0.2 μg per lane. (B) Quantitative analysis of results obtained in (A). The chart shows the ratio of densitometry obtained from the overlay assay to that from the NBB-stained blot. The results are from $n=7$ (GST-c-BSV), $n=6$ (GST-c-SmAV) and $n=3$ (GST) samples in each case. (C, left) NBB stain of total protein on blot before incubation with overlay solution. (C, right) Immunostain with anti-GST antibody after processing with overlay buffer containing 1.25 μg ml^{-1} GST-c-SmAV or GST only as indicated. Purified proteins and their corresponding overlay signals in lanes are indicated with arrowheads. Both recombinant CaP and recombinant calmodulin were at 3 μg per lane. (D) Quantitative analysis of results obtained in (C). The chart shows the ratio of densitometry obtained from the overlay assay to that from the NBB-stained blot. The results are from $n=5$ (CaP) and $n=3$ (CaM) samples for the GST-c-SmAV overlay, and $n=3$ (CaP) and $n=3$ (CaM) samples for the GST overlay. (E) Overlay assay of GST-c-SmAV with chymotrypsin-digested fragments of CaP. (left) NBB stain of blot before incubation with overlay solution. (right) Immunostain with anti-GST antibody after processing with overlay buffer containing 1.25 μg ml^{-1} GST-c-SmAV. Undigested (full-length) and fragments of CaP are indicated with arrowheads. (F) Quantitative analysis of results obtained in (E). The chart shows the ratio of densitometry obtained from the overlay assay to that from the NBB-stained blot. The results are from $n=5$ samples.

Analysis of the SmAV sequence by motif searching programs at high stringency (http://scansite.mit.edu/ and CD Search, NCBI, http://www.ncbi.nlm.nih.gov/Structure/cdd/wrpsb.cgi) revealed several potentially significant regulatory sites. One of the two nuclear targeting sequences (Fig. 2A, blue) within the first insert in skeletal-muscle archvillin (Oh et al., 2003) is conserved in SmAV. C-Terminal sequences homologous to six domains in gelsolin and villin, characteristic of supervillins and archvillins (Pestonjamasp et al., 1997), are also present in SmAV (Fig. 2B, red ovals and short rectangles). Additionally, several kinase-binding sites and phosphorylation sites are predicted (Fig. 2B). Because CaP has been linked with PKC- and ERK-dependent signaling pathways, it is noteworthy that the SmAV sequence predicts the presence of two ERK-binding sites and a motif consistent with phosphorylation by PKC and a proline-directed kinase.

Direct SmAV-CaP binding in vitro

Binding between CaP and SmAV was confirmed by blot overlay assays (Fig. 3). As is shown in Fig. 3A, recombinant CaP from the overlay buffer binds to blotted GST fusion proteins containing the C-terminus of either bovine supervillin (GST-c-BSV, amino acids 1282-1792) or SmAV (GST-c-SmAV, amino acids 1822-2073). Neither protein binds appreciably to equal amounts of GST (Fig. 3A). Quantitative densitometry analysis (Fig. 3B) of the ratio of the CaP immunostained band to that of the total protein band obtained by NBB staining confirms that there is significant binding to both GST-c-BSV and GST-c-SmAV but little binding to GST alone. Specific binding was also observed in the reverse experiment [i.e. overlays with GST-c-SmAV or GST in the overlay buffer and CaP and calmodulin (for comparison) on the blot] (Fig. 3C). Even though as much or more calmodulin was present on the blot, more GST-c-SmAV (as visualized with anti-GST antibody) bound to CaP than to calmodulin (Fig. 3C). By contrast, with an equal amount of GST alone in the overlay buffer, no binding was detected to either CaP or calmodulin on blots, even at long exposures (Fig. 3C). Quantitative analysis (Fig. 3D) of the ratio of the GST immunostained band to that of the total protein band obtained by NBB staining confirmed these observations.

To confirm the domain of CaP responsible for binding to SmAV, purified turkey-gizzard CaP was chymotrypsin digested and fragments were identified by N-terminal sequencing and mass spectrometry (Leinweber et al., 2000). These fragments were used in overlay assays with GST-c-SmAV in the overlay buffer. The results indicate that GST-c-SmAV specifically binds to the 20 kDa fragment and to the undigested full-length CaP, but that the overlay signal with the 14 kDa fragment is almost undetectable (Fig. 3E). The quantitative analysis of the anti-GST-immunostained bands normalized to those for total protein confirms these results (Fig. 3F). The 20 kDa fragment to which GST-c-SmAV bound contains residues 7-152 (Fig. 1B), which encompass the single type-3 CaP-homology (CH) domain of CaP (Gimona et al., 2002).
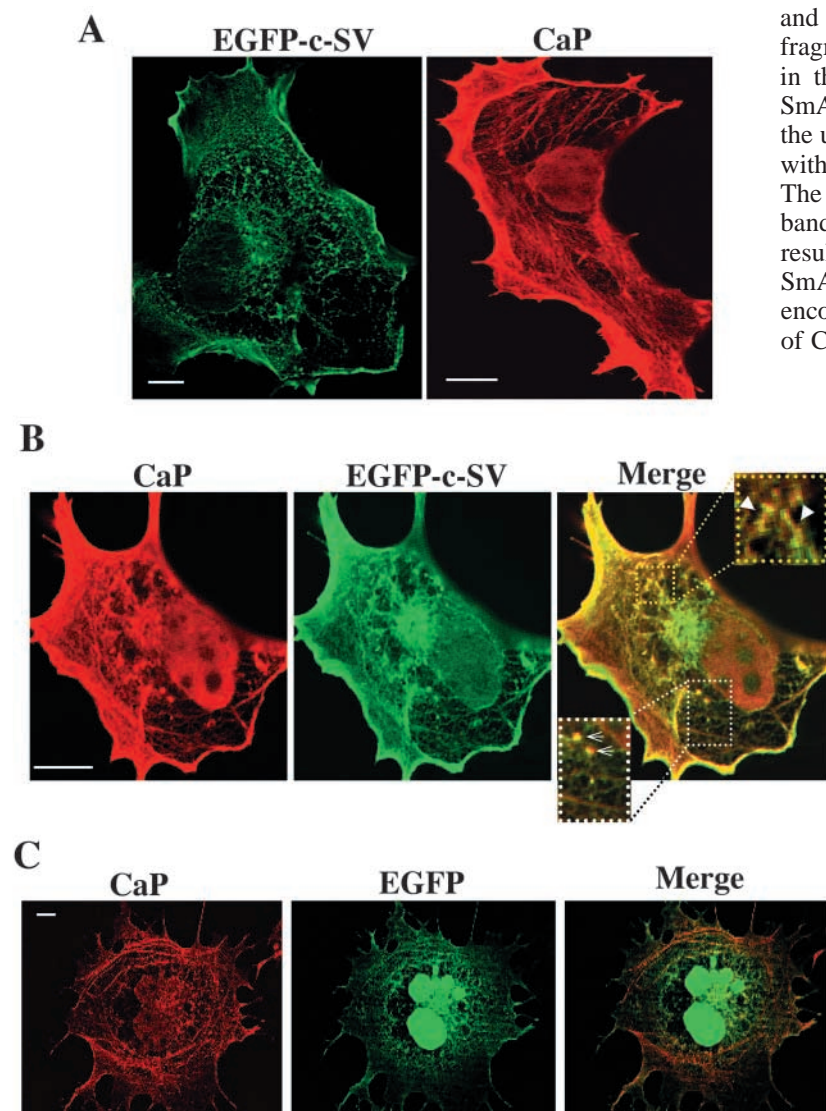
Colocalization in COS-7 cells

To verify the interaction between CaP and supervillin family proteins in vivo, we tested for protein colocalization in COS-7 cells, which are transformed epithelial cells that are easily transfectable with multiple plasmids. We transfected these cells with plasmids encoding His-tagged ferret h1CaP and a previously described C-terminal fragment of bovine supervillin tagged with enhanced green fluorescent protein (EGFP-c-SV, amino acids 1010-1792) (Wulfkuhle et al., 1999). This C-

Fig. 4. CaP and the supervillin C-terminus colocalize in COS-7 cells. Confocal images of immunostained transfected COS-7 cells. (A, left) Single expression of the EGFP-tagged C-terminal 783 residues of bovine supervillin (EGFP-c-SV). (A, right) Single expression of h1-CaP. (B) CaP (left) and EGFP-c-SV (middle) co-expressed in COS-7 cells. Merged image is shown to the right; regions of signal overlap appear in yellow. (C) Co-expression of CaP and EGFP control. CaP was visualized by staining with an anti-CaP antibody and EGFP-c-SV was visualized with an anti-GFP antibody. Scale bar, 10 μm.

Table 1. Calponin and SmAV colocalize significantly in COS-7 cells, and agonist stimulation increases the colocalization coefficient in aorta cells

Cell type	Protein	Mean colocalization coefficient*	s.e.	*P* value
COS-7 cells	Calponin-SmAV	0.79	0.02	–
	Random calponin-SmAV	0.41	0.02	0.0001
	SmAV-calponin	0.72	0.03	–
	Random SmAV-calponin	0.51	0.01	0.0003
Unstimulated FASMCs‡	SmAV-calponin	0.34	0.05	–
	Random SmAV-calponin	0.25	0.01	0.12
	Calponin-SmAV	0.58	0.05	–
	Random calponin-SmAV	0.37	0.03	0.02
FASMCs + phenylephrine	SmAV-Calponin	0.51	0.20	–
	Random SmAV-calponin	0.17	0.01	0.0001
	Calponin-SmAV	0.80	0.02	–
	Random calponin-SmAV	0.23	0.02	0.0001

In each case, 10-25 cells were analysed.
*The proportion of first protein that colocalizes with second protein.
‡FASMCs, ferret-aorta smooth-muscle cells.

terminal bovine supervillin fragment is 94% identical (96% homologous) to ferret SmAV in the region containing the putative CaP-binding site. We used this construct, which lacks the N-terminal sequences of supervillin that interact with F-actin and myosin II (Chen et al., 2003; Wulfkuhle et al., 1999), because CaP also binds actin (Gimona et al., 2002). Thus, colocalization of EGFP-c-SV with CaP associated with actin filaments can be informative in a way that colocalization with full-length SmAV would not be.

CaP and EGFP-c-SV did colocalize in COS-7 cells (Fig. 4). In cells expressing EGFP-c-SV only, this protein was concentrated primarily in cytoplasmic punctae and at the cell periphery (Fig. 4A, left, green). All nine randomly acquired images displayed this qualitative pattern. By contrast, cells expressing exogenous CaP by itself displayed both peripheral (12 out of 13 cells) and linear (13 out of 13 cells) staining (Fig. 4A, right, red), consistent with CaP's association with actin-containing microfilaments (Parker et al., 1998). In cells transfected with both constructs, overlap in staining was observed at punctae reminiscent of cell-substrate adhesion plaques (12 out of 12 cells) (Fig. 4B, inset, arrows) and along short filaments in the cell interior (11 out of 12 cells) (Fig. 4B, inset, arrowheads) as well as at cell peripheries (12 out of 12 cells). Calculation of colocalization coefficients confirms that there is a statistically very significant overlap of CaP with SmAV and of SmAV with CaP, compared with that for the same images when randomized (Table 1).

As a negative control, we co-transfected CaP and the empty EGFP vector (Fig. 4C). As previously reported (Wulfkuhle et al., 1999), EGFP alone labeled the nucleus and little colocalization with CaP was observed. CaP again showed a prominent filamentous staining but EGFP does not (Fig. 4C).

To test more rigorously for colocalization of CaP and EGFP-c-SV, we pre-extracted doubly transfected COS-7 cells with Triton X-100 before fixation and staining. This procedure releases proteins that are unbound or only loosely bound to cytoskeletal structures. As previously reported (Wulfkuhle et al., 1999), essentially all EGFP-c-SV expressed by itself in COS-7 cells was released by pre-extraction with Triton X-100 before cell fixation (Fig. 5A, right, green). By contrast, exogenously expressed CaP continued to exhibit a linear appearance in Triton-extracted cells (Fig. 5B, red). In cells

expressing both CaP and EGFP-c-SV, the extractability of EGFP-c-SV with 0.5% Triton X-100 (Fig. 5C, right, green) and with 0.1% Triton (not shown) was greatly decreased. In these pre-extracted cells, CaP and EGFP-c-SV continued to colocalize extensively in cytoplasmic punctae and along linear structures (presumably microfilaments) even after Triton pre-extraction (Fig. 5C, right, overlap in yellow). These results suggest that CaP stabilizes the association of the supervillin C-terminus with the cytoskeleton and that EGFP-c-SV might potentiate the localization of CaP to cytoplasmic punctae.

Co-fractionation of CaP and SmAV from smooth muscle

The colocalization of overexpressed CaP and EGFP-c-SV in COS-7 cells suggests an interaction between these two proteins but does not necessarily indicate that the endogenous proteins interact in differentiated smooth muscle. As one test of co-association of endogenous SmAV and CaP in differentiated smooth muscle tissue, we fractionated at high speed (165,000 ***g***) both unstimulated smooth-muscle tissue and tissue stimulated for 10 minutes with the agonist, phenylephrine (Fig. 6). Three fractions were obtained: a cytosolic fraction (proteins released by homogenization in the absence of detergent); a Triton-extractable ('membrane') fraction (proteins released with 0.5% Triton X-100); and a Triton-insoluble ('cytoskeletal') fraction (proteins released with 1.2% SDS and 0.5% Triton X-100). In both unstimulated and stimulated tissues, SmAV and CaP co-fractionated in the cytoskeletal fraction (Fig. 6), consistent with an affinity for cytoskeletal structures and/or Triton-insoluble membrane domains.

Agonist-dependent colocalization

To define more precisely the localizations of endogenous SmAV and CaP in differentiated smooth-muscle cells, we performed quantitative confocal imaging studies on freshly isolated cells from the aorta of the ferret (Fig. 7). Using an antibody raised against the N-terminal 340 amino acids of human supervillin (anti-H340) (Nebl et al., 2002), we detected a single band at ~231 kDa in western blots of whole-cell homogenates of ferret aorta (Fig. 7A). The size of this protein is consistent with the size of SmAV predicted from the deduced

Fig. 5. Co-transfection with CaP prevents extraction of EGFP-c-SV by Triton X-100 from COS-7 cells. (A, left) Unextracted COS-7 cell singly transfected with EGFP-c-SV. (A, right) COS-7 cell singly transfected with EGFP-c-SV and extracted with 0.5% Triton X-100 before fixation. (B, left) Unextracted COS-7 cell singly transfected with CaP. (B, right) COS-7 cell singly transfected with CaP and extracted with 0.5% Triton X-100 before fixation. (C, left) Unextracted COS-7 cell co-transfected with EGFP-c-SV (top) and CaP (middle). (C, right) COS-7 cell co-transfected with EGFP-c-SV (top) and CaP (middle) and extracted with 0.5% Triton X-100 before fixation. Merged images shown at the bottom, with regions of overlap in yellow. Scale bar, 10 µm.
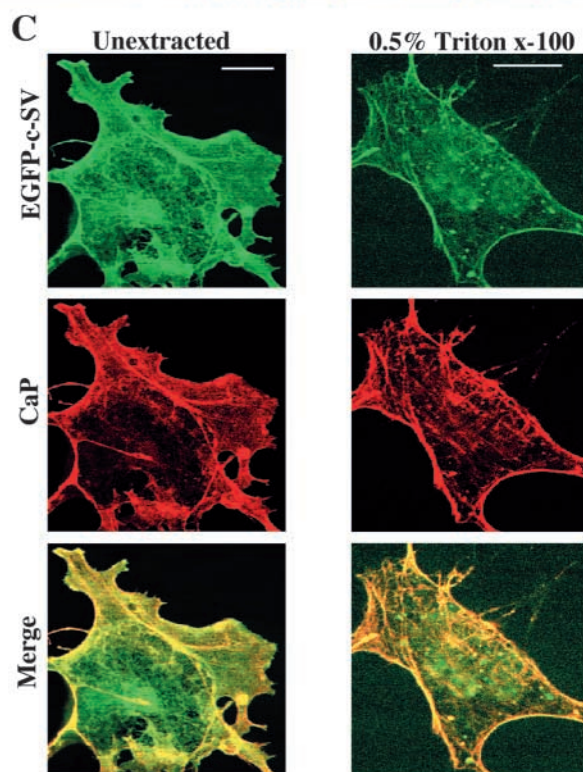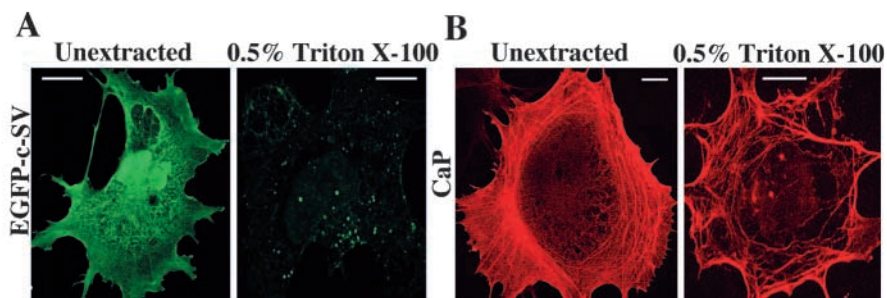
amino acid sequence and suggests that SmAV is the dominant member of the supervillin/archvillin family in aorta smooth muscle. The specificity of this antibody further suggests that it can be used to image SmAV in this tissue.

In images of unstimulated smooth-muscle cells that had been freshly isolated from aortic tissue, we found, as has been previously reported (Parker et al., 1998), that CaP is excluded from the nucleus, localizing primarily to linear structures (Fig. 7B, left, green), presumably microfilament bundles (Parker et al., 1998). These previous studies determined that CaP colocalizes with actin in these bundles (Parker et al., 1998). SmAV also is excluded from the nucleus but, in contrast to CaP, is concentrated in a non-filamentous, more globular, pattern throughout the cell interior (Fig. 7B, middle, red). Some punctate staining at the cell periphery is also detected (arrowheads). A merged image (Fig. 7B, right) of the CaP and SmAV signals shows little convincing overlap. Quantification of colocalization coefficients confirmed that the degree of colocalization is lower than that in the COS-7 cells (Table 1). Furthermore, the proportion of SmAV that overlaps with CaP was not statistically different from that due to chance, as measured in randomized versions of the same images. The

reverse comparison (i.e. the proportion of CaP that overlaps with SmAV), although low, was significantly greater than that for the randomized images. The difference from the random images is presumably due to the fact that the CaP is organized into discrete bundles overlying the more diffuse pattern of SmAV.

Interestingly, a very different pattern emerges when the cells are stimulated with the α-adrenergic agonist phenylephrine (Fig. 7C). As previously reported (Menice et al., 1997), the addition of phenylephrine to ferret aortic cells causes CaP to translocate to the cell periphery (Fig. 7C, left, green). Under these conditions, the SmAV distribution also shifts towards the cell periphery (Fig. 7C, middle, red), where it distributes with CaP (Fig. 7C, right, yellow). This results in an increase in the colocalization coefficients (Table 1). Furthermore, in the presence of phenylephrine, both the overlap of SmAV on CaP and the overlap of CaP on SmAV are significantly greater than that seen in the corresponding randomized images. Ratio analysis also confirms that the individual translocations of each protein to the cell periphery are significant (Fig. 8).

Fig. 6. Tissue fractionation of CaP and SmAV. Immunodetection of SmAV (top) and CaP (bottom) in cytosolic, Triton-X-100-extractable ('membrane') and Triton-X-100-resistant ('cytoskeletal') fractions from unstimulated tissue or from tissue stimulated for 10 minutes with 10^{-5} M phenylephrine.
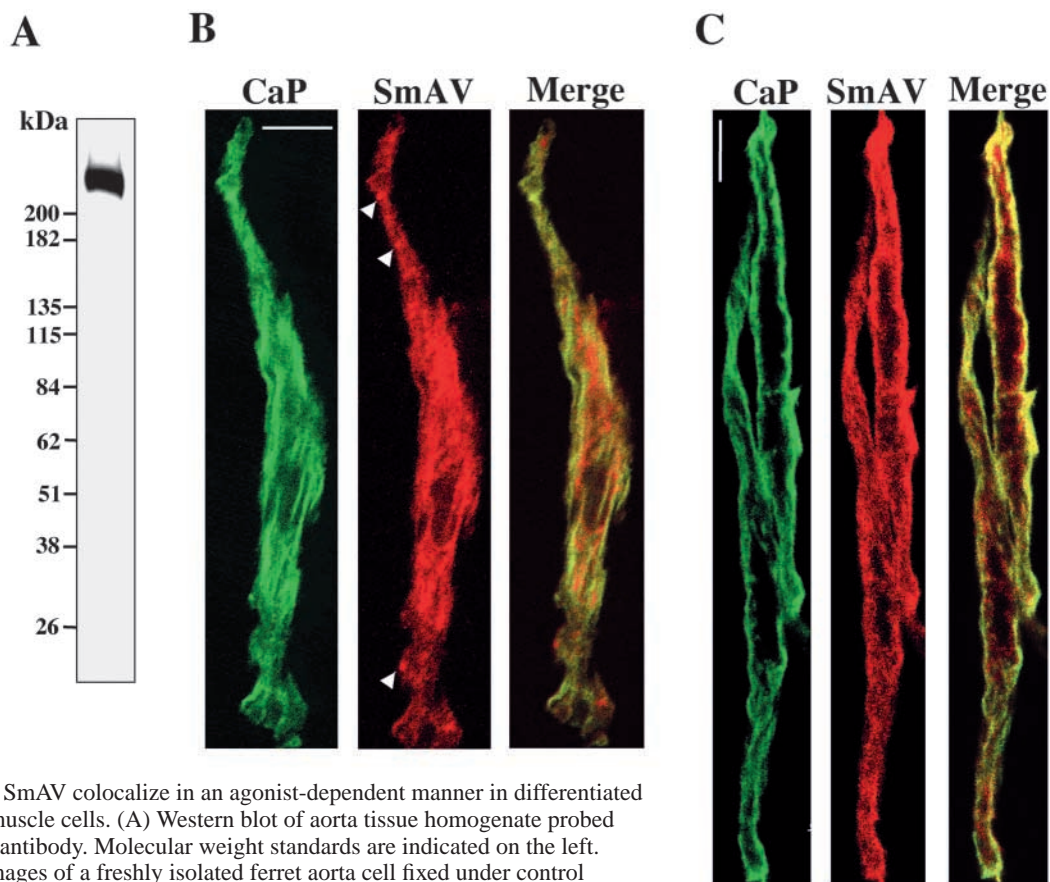
Fig. 7. CaP and SmAV colocalize in an agonist-dependent manner in differentiated aortic smooth-muscle cells. (A) Western blot of aorta tissue homogenate probed with anti-H340 antibody. Molecular weight standards are indicated on the left. (B) Confocal images of a freshly isolated ferret aorta cell fixed under control conditions and labeled for endogenous levels of CaP (left, green) and SmAV (middle, red). Merged images are shown on the right. (C) Confocal images of a freshly isolated ferret aorta cell fixed in the presence of 10^{-5} M phenylephrine for 10 minutes and labeled for CaP and SmAV. Merged images are on the right, with signal overlap in yellow. Scale bar, 10 µm.

CaP and SmAV co-translocate with similar time courses

To confirm the statistical significance of the SmAV redistribution, we performed digital image analysis with an algorithm in which the surface fluorescence is divided by the fluorescence in the cell core (Khalil et al., 1994) (Fig. 8, inset). The phenylephrine-induced translocations of both SmAV and CaP were highly statistically significant (Fig. 8A,B). However, although the average ratios for SmAV and CaP were 1.35 and 1.42, respectively, in unstimulated cells, stimulation caused the ratio for SmAV to increase to 2.22, whereas the ratio for CaP increased to 3.83. These results suggest that a larger proportion of the SmAV remains in the center of the cell.

To test whether SmAV and CaP co-translocate with a similar time course, ratios of SmAV distributions were determined as a function of time after phenylephrine addition (Fig. 8C). SmAV targeting to the cell periphery reaches a maximum within 4 minutes of stimulation, and persists through the 10 minutes of observation. This time course is indistinguishable from that of CaP, as previously determined under similar experimental conditions in the same cell type (Menice et al., 1997).

SmAV knockdown decreases PKC-dependent contractility in vascular tissue

To investigate whether SmAV plays a regulatory role in the contractile function of differentiated smooth muscle similar to that documented previously for CaP (Je et al., 2001), we used an antisense knockdown approach that preserves contractility in organ culture (Fig. 9). We achieved ~50% knockdown of SmAV expression in ferret aorta smooth-muscle tissue (Fig. 9A). By contrast, neither actin nor ERK1/2 total protein values changed with antisense treatment (data not shown). We have previously shown that this method transfects antisense oligonucleotides equally into all cells across the thickness of the tissue preparation (Je et al., 2001). Although no significant change was observed in the magnitude of contractility mediated by depolarization (Fig. 9B), SmAV knockdown led to a significant decrease in the magnitude of contractions triggered by activation of PKC with a phorbol ester (Fig. 9C). Treatment with a randomized version of the nucleotides used in the antisense sequence had no significant effect on the magnitude of either type of contraction, as compared with sham-treated muscles (Fig. 9B-D). Consistent with our previous observations that the proportion of phenylephrine-stimulated contraction that persists in a Ca-free buffer (about one-third of the total contraction) is specifically PKC dependent (Khalil et al., 1994; Menice et al., 1997), we found that calcium-independent, phenylephrine-induced contractions were also significantly reduced by SmAV knockdown (Fig. 9D). This phenotype, with respect to both phorbol-ester- and
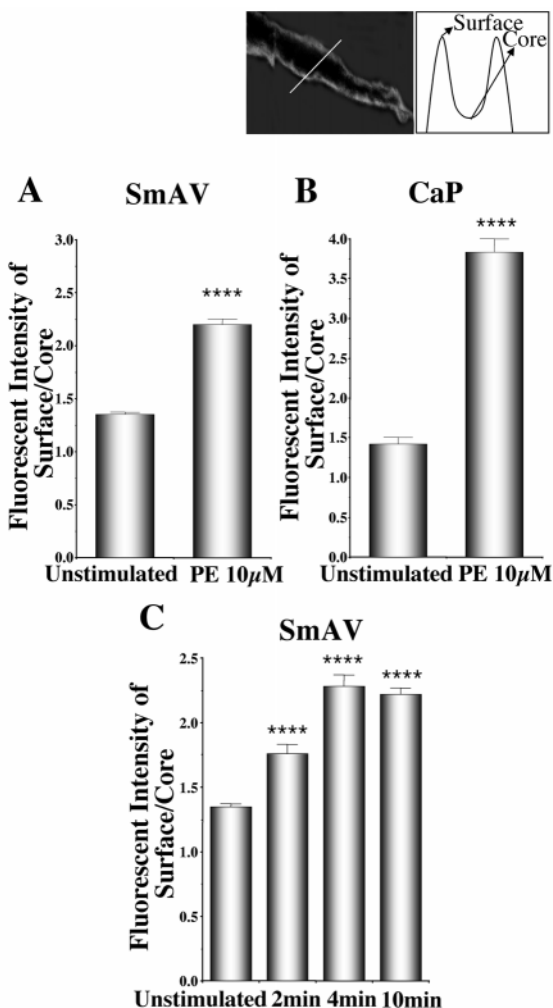
Fig. 8. Quantification of subcellular distribution of CaP and SmAV in differentiated smooth-muscle cells. Fluorescence intensities were quantified from confocal micrographs. In all cases, between 14 and 53 cells were analysed. (Inset) Method used to produce line scans for quantification of ratios. (A) Comparison of the average (with standard error) of surface:core ratios for the distribution of SmAV in the absence and presence of phenylephrine (PE). (B) Comparison of the average surface:core ratios for the distribution of CaP in the absence and presence of PE. (C) Average ratios (+ s.e.m.) of SmAV surface-membrane to cytosol fluorescence intensities in single smooth-muscle cells that were unstimulated or stimulated with PE for 2 minutes, 4 minutes or 10 minutes. ****$P<0.0001$ compared with unstimulated values.

Ca-independent phenylephrine-stimulated contractions, is essentially identical to that observed for CaP knockdown in this tissue (Je et al., 2001). Finally, even though (as mentioned above) total ERK1/2 protein levels do not change with antisense treatment, SmAV knockdown inhibits PKC-mediated activation of both ERK1 and ERK2 (Fig. 9E), as detected with an anti-phospho-ERK1/2 antibody. A similar inhibition of PKC-induced ERK1/2 activation has also been observed after CaP knockdown (Je et al., 2001). These results implicate SmAV in both PKC-dependent contractility and signaling to ERK1/2.

Localization to the cell cortex

To define further the intracellular site(s) at or near the plasma membrane to which SmAV and CaP relocate after activation of PKC, we immunolocalized endogenous levels of these proteins in cultured A7r5 vascular smooth muscle cells before (Fig. 10A) and after (Fig. 10B) treatment with a phorbol ester, PDBu. The spread morphology of these cells facilitates resolution of subcellular localizations especially between diverse membrane domains. Phorbol-ester treatment of these cells induces a disassembly of actin filament bundles and the concomitant appearance of podosome-like, tubular structures containing F-actin, myosin II and other cytoskeletal proteins that arise from the ventral cell surface and protrude several micrometers into the cell cytoplasm (Brandt et al., 2002; Fultz and Wright, 2003; Hai et al., 2002; Kaverina et al., 2003). In untreated cells, SmAV is localized to membrane ruffles and non-filamentous structures in the cell interior (Fig. 10Aa). CaP is localized primarily to F-actin-containing filaments (Fig. 10Ag,k). In PDBu-treated A7r5 cells (Fig. 10B), we found that endogenous SmAV colocalizes with F-actin (Fig. 10Ba-c) and endogenous h1 CaP (Fig. 10Bg-i) at podosomes (arrowheads) and membrane ruffles (arrows). Podosomes also contain nonmuscle myosin IIB (Fig. 10Bd-f) and ERK1/2 (Fig. 10Bj-l). Because the antibodies used in this study are specific on immunoblots (not shown), these results suggest that PKC induces the relocation of SmAV, CaP, nonmuscle myosin IIB and ERK1/2 to podosome-like structures at or near the plasma membranes of vascular smooth-muscle cells. The phenylephrine-induced shifts in protein distributions in A7r5 cells (Fig. 10) are qualitatively similar to those observed in the differentiated aortic smooth-muscle cells (Figs 7, 8), suggesting that the peripheral distribution of SmAV and CaP in the aortic cells might arise from an abundance of similar podosome-like structures (i.e. complexes containing both membrane and cytoskeletal components).

Discussion

This paper describes for the first time a smooth-muscle isoform of supervillin. This isoform (SmAV) was identified as an interacting protein with CaP in a yeast two-hybrid assay. We have verified this interaction using both in vitro and in vivo techniques, including functional assays. SmAV appears to be the predominant supervillin/archvillin homolog in smooth muscle, because western blots of smooth-muscle homogenates with an antibody against supervillin show only a single band at the expected molecular mass of SmAV. Furthermore, only a single RT-PCR product was found for each primer pair during the cloning of the cDNA.

It is noteworthy that the SmAV sequence contains several predicted nuclear targeting sequences and yet imaging of differentiated smooth muscle cells clearly indicates an absence of SmAV from the nucleus in both stimulated and unstimulated cells. By contrast, supervillin (Pestonjamasp et al., 1997) and skeletal-muscle archvillin (Oh et al., 2003) can exhibit strong nuclear localization. This apparent difference in the isoforms might be explained by a retention of SmAV in the cytoplasm by virtue of its interaction with CaP and/or with other smooth-muscle cytoskeletal elements.

SmAV associates with CaP biochemically and functionally. We observe SmAV-CaP interactions in reciprocal yeast two-
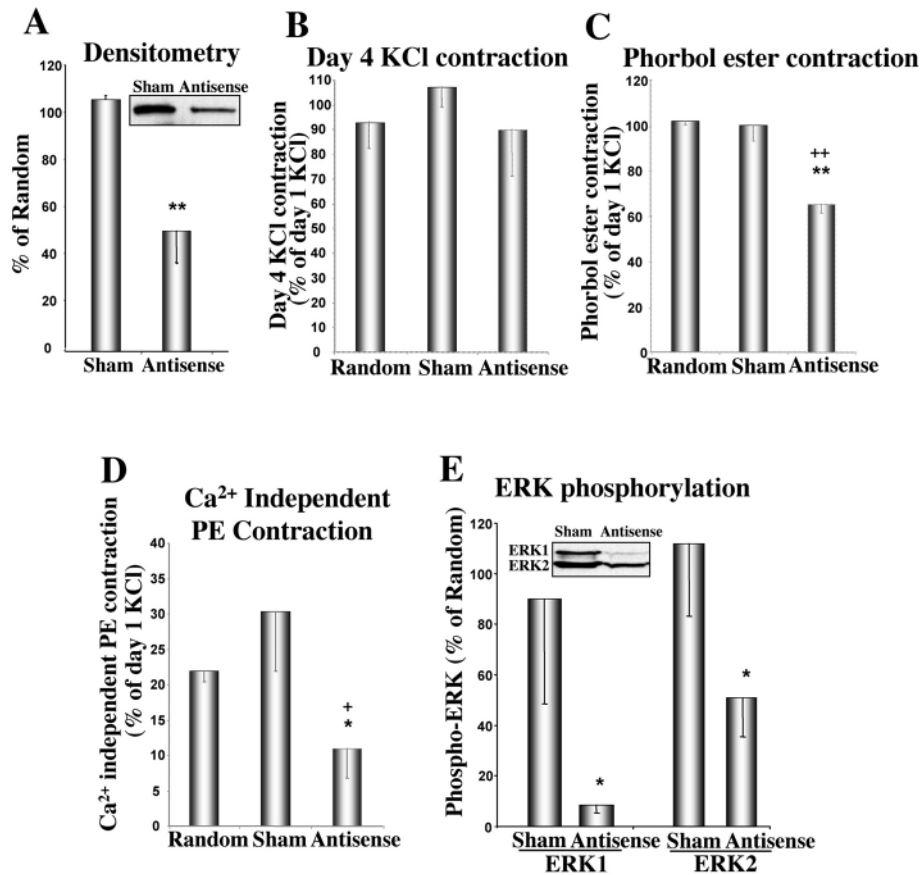
Fig. 9. Antisense knockdown of SmAV decreases contractility and signaling in smooth-muscle tissue. (A) Densitometric analysis of SmAV protein levels from immunoblots of antisense- and sham-treated muscles expressed as a precentage of random loaded tissue. **$P \leq 0.01$. (Inset) A typical western blot for SmAV. (B) Magnitude of steady-state contraction in response to a depolarizing physiological saline solution containing 51 mM KCl. Forces are normalized to the amplitude of contraction of each muscle in response to 51 mM KCl physiological saline solution on day 1. (C) Contraction of muscle strips in response to the phorbol ester DPBA (3 μM). Forces are normalized to the amplitude of contraction of each muscle in response to 51 mM KCl on day 1. **$P \leq 0.01$ for antisense compared with sham; ++$P \leq 0.001$ for antisense compared with random. (D) Contraction of muscle strips in response to 10 μM phenylephrine in the absence of extracellular calcium. Forces are normalized to the amplitude of contraction of each muscle in response to 51 mM KCl physiological saline on day 1. *$P \leq 0.05$ for antisense compared with sham; +$P \leq 0.05$ for antisense compared with random. (E) Densitometric analysis of phospho-ERK1/2 on immunoblots for antisense- or sham-treated muscles exposed to DPBA, normalized to that for muscles treated with a random sequence. (Inset) A typical western blot for phospho-ERK1/2. **$P \leq 0.05$. All values are from between three and five separate experiments.

hybrid assays, direct binding on reciprocal blot overlays and colocalization in doubly transfected COS-7 cells. Endogenous SmAV and CaP co-translocate with similar kinetics in response to PKC-stimulating agonists in freshly isolated cells from smooth muscle, and are co-extracted in the detergent-resistant cytoskeletal fraction from this tissue. Endogenous SmAV and CaP also are co-targeted with ERK1/2 to PKC-induced 'podosome-like' structures in A7r5 cells. Finally, antisense knockdown of SmAV inhibits stimulus-mediated contraction through a signaling pathway that is indistinguishable from that previously described for CaP (Je et al., 2001).

Because CaP and supervillin/archvillin both contain binding sites for F-actin and/or myosin II (Chen et al., 2003; Gimona et al., 2002; Gusev, 2001), it is important to realize that the interaction described here does not require the presence of either actin or myosin. Interactions were observed both in vitro with purified recombinant proteins and in vivo, when CaP was co-transfected into COS-7 cells with an EGFP-tagged chimeric protein containing the CaP-binding domain of supervillin but lacking interaction sites for F-actin or myosin II.

By contrast, the co-fractionation of SmAV and CaP in a cytoskeletal/detergent-resistant fraction in both resting and stimulated tissues is consistent with multiple cytoskeletal associations and might reflect a regulatory role for these proteins during actin- and myosin-mediated contractility. Detergent-resistant cell fractions contain many components, including cholesterol-rich membrane domains such as those containing caveolin and other lipid-raft-organizing components, as well as cytoskeletal proteins. In fact,

supervillin and skeletal-muscle archvillin associate closely with both lipid-raft-organizing proteins and cytoskeletal elements (Nebl et al., 2002).

The agonist-stimulated translocation of endogenous SmAV and CaP to the cell periphery in both differentiated smooth-muscle cells and A7r5 cells further suggests a role for these proteins in mediating interactions between the cortical membrane skeleton and the contractile apparatus. CaP has previously been reported to translocate from contractile filaments containing α-actin to the β-actin containing network of the submembranous cortex (Parker et al., 1998). Thus, we suggest that CaP and SmAV translocate from different sites within the cell to a common cytoskeletal structure that is in contact with a detergent-resistant component of the cell membrane.

The peripheral localization of CaP and SmAV in differentiated smooth-muscle cells might reflect a recruitment into structures analogous to the 'podosome-like structures' in immortalized A7r5 cultured cells, to which CaP and SmAV also colocalize after PKC activation by PDBu. Podosomes are actin- and myosin-II-associated tubular invaginations of the basal surface of the plasma membrane that have been implicated in remodeling of the cortical actin cytoskeleton (Brandt et al., 2002; Fultz et al., 2000; Gimona et al., 2003; Fultz and Wright, 2003; Li et al., 2001). They also contain α-actinin, vinculin and transfected h2 CaP (Gimona et al., 2003; Hai et al., 2002). However, in the same study (Gimona et al., 2003), h1 CaP transfected into these cells was not detected in podosomes even though displacement of CaP from actin
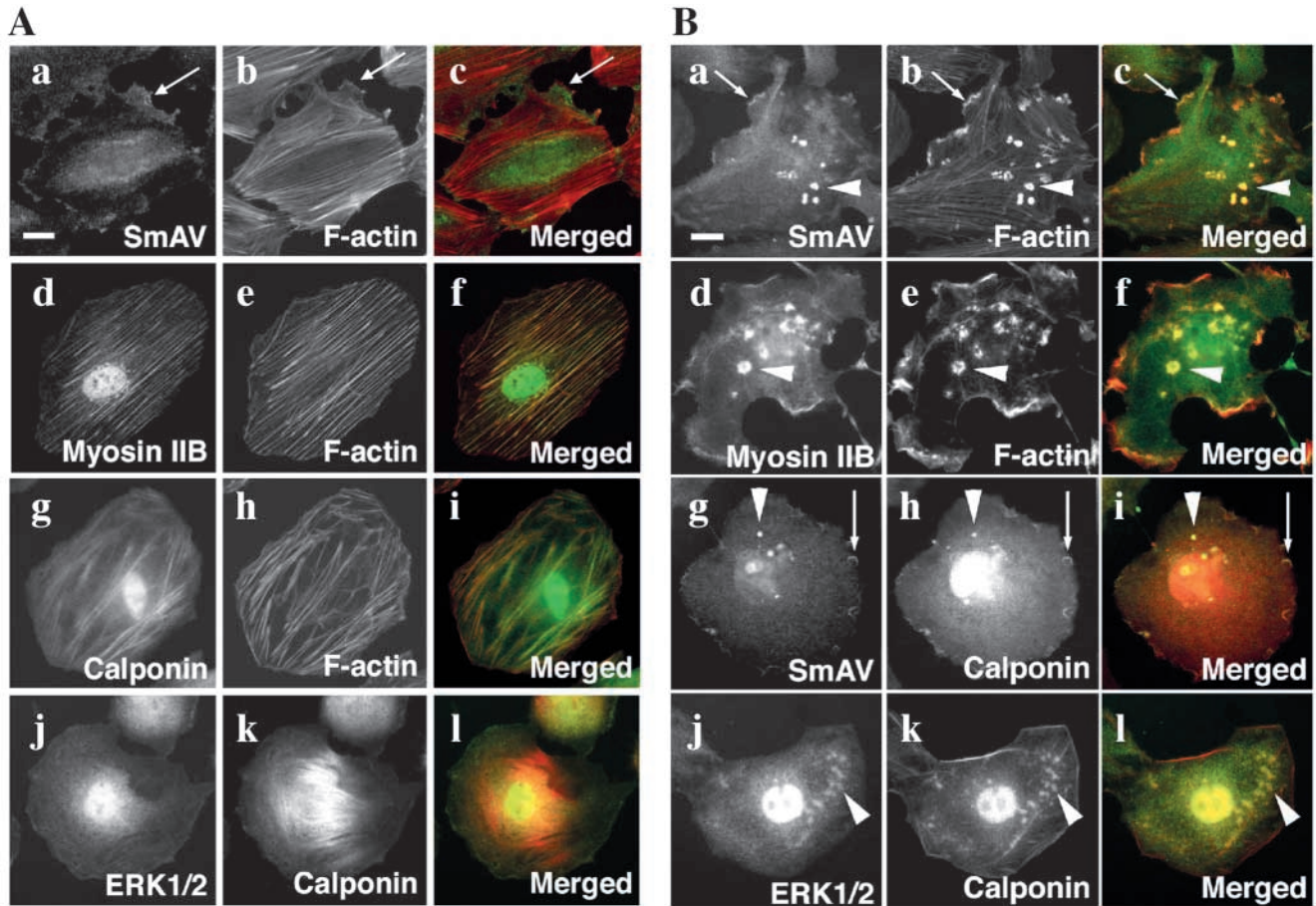
Fig. 10. Localization of endogenous SmAV, F-actin, nonmuscle myosin II, CaP and ERK1/2 before and after PDBu treatment of A7r5 smooth-muscle cells. (A) In untreated A7r5 cells, endogenous SmAV (a) appears to be membranous, whereas F-actin (b,e,h), nonmuscle myosin II (d) and CaP (g,k) are primarily associated with microfilaments, and ERK1/2 appears to be cytosolic (j). (B) After PKC activation with PDBu, endogenous SmAV (a,g), F-actin (b,e), nonmuscle myosin II (d), CaP (h,k) and ERK1/2 (j) all localize to podosome-like structures (arrowheads). SmAV, F-actin, myosin IIB and CaP also concentrate at or near membrane ruffles (arrows). Merged images (c,f,i,l) show the overlap of signal from panels on the left (green) with the signal from the middle panels (red); the overlap appears yellow. Scale bar, 25 μm.

filaments is thought to be a prerequisite for podosome formation (Burgstaller and Gimona, 2004). Interestingly, we found that endogenous h1 CaP is indeed localized to the podosomes. Perhaps the dynamics of h1 CaP distribution change when h1 CaP levels increase after transfection.

This is the first report of which we are aware for the localization of supervillin, archvillin, endogenous h1 CaP or ERK1/2 to these podosome-like structures. Hai et al. have suggested that podosomes represent molecular scaffolds for PKC-mediated effects leading to Ca^{2+} sensitization in smooth muscle (Hai et al., 2002). Because the targeting of ERK to the cell periphery is PKC dependent and associated with Ca^{2+} sensitization in smooth muscle (Collins et al., 1992; Khalil et al., 1995), our demonstration of PDBu-mediated recruitment of ERK1/2 to podosomes supports this hypothesis.

The specific interaction between SmAV and the CH domain of CaP is interesting because this domain is known to bind ERK (Leinweber et al., 1999). However, the N-terminal end of SmAV is predicted to contain ERK binding and phosphorylation sites. This raises the possibility that the binding of the CH domain of CaP to SmAV might displace

ERK1/2 from CaP and free ERK to interact with SmAV or other proteins in the podosome.

The question arises of the mechanism by which CaP/SmAV downregulation leads to the observed inhibition of contractility. CaP has been previously suggested to function as an adapter protein to facilitate the targeting of PKC and ERK1/2 to a signaling complex in the cell cortex (Leinweber et al., 2000; Menice et al., 1997). Once CaP, ERK1/2 and SmAV arrive at the cell cortex, SmAV might displace ERK1/2 from CaP, allowing ERK to be activated by the upstream kinase, MEK. Subsequent ERK1/2-mediated phosphorylation of caldesmon at Ser-789 might then relieve the caldesmon-mediated inhibition of actomyosin interactions (Sobue et al., 1982). In this model, the absence of either SmAV or CaP inhibits ERK-dependent effects but has little or no effect on contractility triggered by calcium-dependent signaling events. It is worth noting that the peak of myosin light chain phosphorylation in this tissue occurs by 1 minute after phenylephrine stimulation and then declines (Menice et al., 1997), preceding the maximal translocation of SmAV (at 4 minutes). Thus myosin phosphorylation pathways might predominate during the

onset of smooth muscle contractions, whereas caldesmon phosphorylation might play a greater role in the sustained increase in contractility. The presence of predicted ERK-binding motifs and proline-directed phosphorylation sites in SmAV further suggests that interactions with membrane and/or cytoskeletal proteins might be under feedback regulatory control from an ERK pathway.

Finally, the phorbol-ester-induced colocalization of CaP and SmAV with ERK to podosomes might imply a role for these or analogous cortical signaling structures in the regulation of MAPKs in general. Thus, this paper might provide a 'missing link' between previous work documenting the importance of the MAPK cascade to early myogenesis of C2C12 cells (Bennett and Tonks, 1997; Cuenda and Cohen, 1999; Weston et al., 2003) and results showing a dominant-negative effect of archvillin sequences on C2C12 myogenesis (Oh et al., 2003). Thus, the stimulus-triggered targeting of CaP and SmAV to the cell cortex might participate in both the regulation of contractility and the coordination of cortical signaling pathways in differentiated and proliferative muscle cells.

References

Altschul, S. F., Madden, T. L., Schäffer, A. A., Zhang, J., Zhang, Z., Miller, W. and Lipman, D. J. (1997). Gapped BLAST and PSI-BLAST: a new generation of protein database search programs. *Nucleic Acids Res.* **25**, 3389-3402.

Bennett, A. M. and Tonks, N. K. (1997). Regulation of distinct stages of skeletal muscle differentiation by mitogen-activated protein kinases. *Science* **278**, 1288-1291.

Brandt, D., Gimona, M., Hillmann, M., Haller, H. and Mischak, H. (2002). Protein kinase C induces actin reorganization via a Src- and Rho-dependent pathway. *J. Biol. Chem.* **277**, 20903-20910.

Burgstaller, G. and Gimona, M. (2004). Actin cytoskeleton remodelling via local inhibition of contractility at discrete microdomains. *J. Cell Sci.* **117**, 223-231.

Carpenter, G. (2000). The EGF receptor: a nexus for trafficking and signaling. *BioEssays* **22**, 697-707.

Chen, Y., Takizawa, N., Crowley, J. L., Oh, S. W., Gatto, C. L., Kambara, T., Sato, O., Li, X.-D., Ikebe, M. and Luna, E. J. (2003). F-Actin and myosin II binding domains in supervillin. *J. Biol. Chem.* **278**, 46094-46106.

Collins, E. M., Walsh, M. P. and Morgan, K. G. (1992). Contraction of single vascular smooth muscle cells by phenylephrine at constant [Ca^{2+}]$_i$. *Am. J. Physiol. Heart Circ. Physiol.* **262**, H754-H762.

Cuenda, A. and Cohen, P. (1999). Stress-activated protein kinase-2/p38 and a rapamycin-sensitive pathway are required for C2C12 myogenesis. *J. Biol. Chem.* **274**, 4341-4346.

Feliciello, A., Gottesman, M. E. and Avvedimento, E. V. (2001). The biological functions of A-kinase anchor proteins. *J. Mol. Biol.* **308**, 99-114.

Fultz, M. E. and Wright, G. L. (2003). Myosin remodelling in the contracting A7r5 smooth muscle cell. *Acta Physiol. Scand.* **177**, 197-205.

Fultz, M. E., Li, C., Geng, W. and Wright, G. L. (2000). Remodeling of the actin cytoskeleton in the contracting A7r5 smooth muscle cell. *J. Muscle Res. Cell Motil.* **21**, 775-787.

Ge, L., Ly, Y., Hollenberg, M. and DeFea, K. (2003). A beta-arrestin-dependent scaffold is associated with prolonged MAPK activation in pseudopodia during protease-activated receptor-2-induced chemotaxis. *J. Biol. Chem.* **278**, 34418-34426.

Gerthoffer, W. T. and Gunst, S. J. (2001). Focal adhesion and small heat shock proteins in the regulation of actin remodeling and contractility in smooth muscle. *J. Appl. Physiol.* **91**, 963-972.

Gimona, M., Djinovic-Carugo, K., Kranewitter, W. J. and Winder, S. J. (2002). Functional plasticity of CH domains. *FEBS Lett.* **513**, 98-106.

Gimona, M., Kaverina, I., Resch, G. P., Vignal, E. and Burgstaller, G. (2003). Calponin repeats regulate actin filament stability and formation of podosomes in smooth muscle cells. *Mol. Biol. Cell* **14**, 2482-2491.

Gusev, N. B. (2001). Some properties of caldesmon and calponin and the participation of these proteins in regulation of smooth muscle contraction and cytoskeleton formation. *Biochemistry* **66**, 1112-1121.

Hai, C. M., Hahne, P., Harrington, E. O. and Gimona, M. (2002). Conventional protein kinase C mediates phorbol-dibutyrate-induced cytoskeletal remodeling in A7r5 smooth muscle cells. *Exp. Cell Res.* **280**, 64-74.

Harnett, K. M. and Biancani, P. (2003). Calcium-dependent and calcium-independent contractions in smooth muscles. *Am. J. Med.* **115**, S24-S30.

Je, H. D., Gangopadhyay, S. S., Ashworth, T. D. and Morgan, K. G. (2001). Calponin is required for agonist-induced signal transduction – evidence from an antisense approach in ferret smooth muscle. *J. Physiol.* **537**, 567-577.

Jiang, M. J. and Morgan, K. G. (1989). Agonist-specific myosin phosphorylation and intracellular calcium during isometric contractions of arterial smooth muscle. *Pflügers Archiv.* **413**, 637-643.

Kaverina, I., Stradal, T. E. and Gimona, M. (2003). Podosome formation in cultured A7r5 vascular smooth muscle cells requires Arp2/3-dependent de-novo actin polymerization at discrete microdomains. *J. Cell Sci.* **116**, 4915-4924.

Khalil, R. A., Lajoie, C. and Morgan, K. G. (1994). In situ determination of the [Ca^{2+}]$_i$ threshold for translocation of the alpha protein kinase C isoform. *Am. J. Physiol., Cell Physiol.* **266**, C1544-C1551.

Khalil, R. A., Menice, C. B., Wang, C.-L. A. and Morgan, K. G. (1995). Phosphotyrosine-dependent targeting of mitogen-activated protein kinase in differentiated contractile vascular cells. *Circ. Res.* **76**, 1101-1108.

Kim, I., Je, H. D., Gallant, C., Zhan, Q., Riper, D. V., Badwey, J. A., Singer, H. A. and Morgan, K. G. (2000). Ca^{2+}-calmodulin-dependent protein kinase II-dependent activation of contractility in ferret aorta. *J. Physiol.* **526**, 367-374.

Laemmli, U. K. (1970). Cleavage of structural proteins during the assembly of the head of bacteriophage T4. *Nature* **227**, 680-685.

Leinweber, B. D., Leavis, P. C., Grabarek, Z., Wang, C.-L. A. and Morgan, K. G. (1999). Extracellular regulated kinase (ERK) interaction with actin and the calponin homology (CH) domain of actin-binding proteins. *Biochem. J.* **344**, 117-123.

Leinweber, B., Parissenti, A. M., Gallant, C., Gangopadhyay, S. S., Kirwan-Rhude, A., Leavis, P. C. and Morgan, K. G. (2000). Regulation of protein kinase C by the cytoskeletal protein calponin. *J. Biol. Chem.* **275**, 40329-40336.

Li, C., Fultz, M. E., Parkash, J., Rhoten, W. B. and Wright, G. L. (2001). Ca^{2+}-dependent actin remodeling in the contracting A7r5 cell. *J. Muscle Res. Cell Motil.* **22**, 521-534.

Menice, C. B., Hulvershorn, J., Adam, L. P., Wang, C. A. and Morgan, K. G. (1997). Calponin and mitogen-activated protein kinase signaling in differentiated vascular smooth muscle. *J. Biol. Chem.* **272**, 25157-25161.

Miller, W. E. and Lefkowitz, R. J. (2001). Expanding roles for beta-arrestins as scaffolds and adapters in GPCR signaling and trafficking. *Curr. Opin. Cell Biol.* **13**, 139-145.

Moreland, S. J., Nishimura, J., van Breemen, C., Ahn, H. Y. and Moreland, R. S. (1992). Transient myosin phosphorylation at constant Ca^{2+} during agonist activation of permeabilized arteries. *Am. J. Physiol.* **263**, C540-C544.

Morgan, K. G. and Gangopadhyay, S. S. (2001). Cross-bridge regulation by thin filament-associated proteins. *J. Appl. Physiol.* **91**, 953-962.

Nebl, T., Pestonjamasp, K. N., Leszyk, J. D., Crowley, J. L., Oh, S. W. and Luna, E. J. (2002). Proteomic analysis of a detergent-resistant membrane skeleton from neutrophil plasma membranes. *J. Biol. Chem.* **277**, 43399-43409.

Oh, S. W., Pope, R. K., Smith, K. P., Crowley, J. L., Nebl, T., Lawrence, J. B. and Luna, E. J. (2003). Archvillin, a muscle-specific isoform of supervillin, is an early expressed component of the costameric membrane skeleton. *J. Cell Sci.* **116**, 2261-2275.

Parker, C. A., Takahashi, K., Tang, J. X., Tao, T. and Morgan, K. G. (1998). Cytoskeletal targeting of calponin in differentiated, contractile smooth muscle cells of the ferret. *J. Physiol.* **508**, 187-198.

Pestonjamasp, K., Amieva, M. R., Strassel, C. P., Nauseef, W. M., Furthmayr, H. and Luna, E. J. (1995). Moesin, ezrin, and p205 are actin-binding proteins associated with neutrophil plasma membranes. *Mol. Biol. Cell* **6**, 247-259.

Pestonjamasp, K. N., Pope, R. K., Wulfkuhle, J. D. and Luna, E. J. (1997). Supervillin (p205): a novel membrane-associated, F-actin-binding protein in the villin/gelsolin superfamily. *J. Cell Biol.* **139**, 1255-1269.

Pfitzer, G. (2001). Regulation of myosin phosphorylation in smooth muscle. *J. Appl. Physiol.* **91**, 497-503.

Pouysségur, J. and Lenormand, P. (2003). Fidelity and spatio-temporal control in MAP kinase (ERKs) signalling. *Eur. J. Biochem.* **270**, 3291-3299.

Pryciak, P. M. (2001). MAP kinases bite back. *Dev. Cell* **1**, 449-451.

Sim, A. T. and Scott, J. D. (1999). Targeting of PKA, PKC and protein phosphatases to cellular microdomains. *Cell Calcium* **26**, 209-217.

Small, J. V. and Gimona, M. (1998). The cytoskeleton of the vertebrate smooth muscle cell. *Acta Physiol. Scand.* **164**, 341-348.

Sobue, K., Morimoto, K., Inui, M., Kanda, K. and Kakiuchi, S. (1982). Control of actin-myosin interaction of gizzard smooth muscle by calmodulin and caldesmon-linked flip-flop mechanism. *Biomed. Res.* **3**, 188-196.

Somlyo, A. P. and Somlyo, A. V. (2003). Ca^{2+} sensitivity of smooth muscle and nonmuscle myosin II: modulated by G proteins, kinases, and myosin phosphatase. *Physiol. Rev.* **83**, 1325-1358.

Swaffield, J. C. and Johnston, S. A. (2003). *Affinity Purification of Proteins Binding to GST Fusion Proteins*. Indianapolis, IN: John Wiley & Sons.

Takahashi, K., Hiwada, K. and Kokubu, T. (1986). Isolation and characterization of a 34000-Dalton calmodulin- and F-actin-binding protein from chicken gizzard smooth muscle. *Biochem. Biophys. Res. Commun.* **141**, 20-26.

Ting, H. J., Yeh, S., Nishimura, K. and Chang, C. (2002). Supervillin associates with androgen receptor and modulates its transcriptional activity. *Proc. Natl. Acad. Sci. USA* **99**, 661-666.

Wang, C. L. (2001). Caldesmon and smooth-muscle regulation. *Cell Biochem. Biophys.* **35**, 275-288.

Weston, A. D., Sampaio, A. V., Ridgeway, A. G. and Underhill, T. M. (2003). Inhibition of p38 MAPK signaling promotes late stages of myogenesis. *J. Cell Sci.* **116**, 2885-2893.

Wier, W. G. and Morgan, K. G. (2003). alpha(1)-Adrenergic signaling mechanisms in contraction of resistance arteries. *Rev. Physiol. Biochem. Pharmacol*. **150**, 91-139.

Winder, S. J., Allen, B. G., Clement-Chomienne, O. and Walsh, M. P. (1998). Regulation of smooth muscle actin-myosin interaction and force by calponin. *Acta Physiol. Scand.* **164**, 415-426.

Wulfkuhle, J. D., Donina, I. E., Stark, N. H., Pope, R. K., Pestonjamasp, K. N., Niswonger, M. L. and Luna, E. J. (1999). Domain analysis of supervillin, an F-actin bundling plasma membrane protein with functional nuclear localization signals. *J. Cell Sci.* **112**, 2125-2136.

Zamir, E. and Geiger, B. (2001). Molecular complexity and dynamics of cell-matrix adhesions. *J. Cell Sci.* **114**, 3583-3590.